Dynamics of Fan-Duct-Plenum Systems in Large-Amplitude Oscillation

H. Matsuo,* K. Fujiwara† and K. Mashima†
Kumamoto University, Kumamoto, Japan
and
K. Matsuo‡
Kumamoto Institute of Technology, Kumamoto, Japan

The dynamic response of the fan-duct-plenum system is investigated. Nonlinear aerodynamic equations for the duct flow are solved using the method of characteristics and connecting the solution with the operating characteristics of the fan, the power plant, and the cushion. The results are compared with those for the lumped-inertance model. The two results are nearly identical in the small-amplitude-low-frequency range. In the higher-frequency range with the large amplitude, the wave effect in the duct flow becomes conspicuous. It tends to relax the lumped-inertance effect. The numerical result is also compared with that obtained by the forced-oscillation test. In the lower-frequency range, the lumped-inertance analysis is sufficient. However, it produces too much pressure variation in the higher-frequency range. The difference in the phase lag also becomes noticeable. The theoretical result is improved by considering the wave effect and approaches the experimental result.

Nomenclature

a = sound velocity
C = peripheral length of the effective cushion area
C_d = discharge coefficient
d = duct diameter
f = frequency of oscillation
H = depth of plenum chamber
h = hoverheight
h_e = hoverheight in the equilibrium condition
J_f = moment of inertia of the fan
J_p = moment of inertia of the power plant
K = coefficient that takes 1 or -1
L_d = duct length
M_{in} = mass flow rate into the cushion
M_{out} = mass flow rate out of the cushion
n_f = rotational speed of the fan
n_p = rotational speed of the power plant
P = pressure (absolute)
P_c = cushion pressure (absolute)
P_d = absolute pressure at the duct exit
P_f = absolute pressure (static) behind the fan
P_i = absolute pressure at the duct entrance
P_0 = atmospheric pressure
Q_f = volume flow rate of fan
S = effective base area of the cushion
S_f = duct sectional area (assumed to be equal to the fan exit area)
T = period of oscillation
T_f = input torque of the fan
T_p = output torque of the power plant
T_{sf} = actual torque of the fan
T_{sp} = actual torque of the power plant
u = fluid velocity
u_d = air velocity at the duct exit
u_i = velocity at the duct entrance
V = cushion volume
β = wall friction coefficient
Δh = amplitude of oscillation
γ = ratio of specific heats
ζ = duct loss coefficient
η_t = transmission efficiency
κ = reduction ratio
λ = $16T_f/(\rho_0\pi^3 d^5 n_f^2)$
ξ = $4Q_f/(\pi^2 d^3 n_f)$
ρ = air density
ρ_c = air density in the cushion
ρ_d = density at the duct exit
ρ_0 = atmospheric density
ϕ = parameter assigning the operation condition of power plant
ψ = $2P_f/(\rho_0\pi^2 d^2 n_f^2)$

I. Introduction

WE previously presented a linear and quasistatical analysis[1] of the stability of air cusions. It was thereafter extended to the nonlinear analysis of large-amplitude oscillations.[2] The result of the analysis was compared with that of the forced-oscillation test. The agreement between the two results was remarkably close, except for the high-frequency range over 1 Hz. The inertial effect (the inertance) of the air in the ducting was further considered in the later study.[3,4] It noticeably improved the result in the frequency range around 1 Hz. It was suggested, however, that in the higher-frequency range other unsteady effects such as the unsteady operation of fans and the wave propagation phenomena in the duct flow would probably become important.

Unsteady effects in the fan-duct system have been investigated by several researchers. Yano and Nagayama[5] investigated the dynamic effect on a fan-duct flow in the scavenging system of the diesel engine. A turbofan and the ducting with a surging tank were considered. The results suggested that the quasistatic characteristics of the fan was sufficient in the fluctuation frequency up to 10 Hz unless the surging occurred. They also suggested that the consideration of the inertance of the air in the duct flow was important, but the wave propagation phenomena were negligible except for the high-frequency

Received Oct. 10, 1986; revision received May 1, 1988.

*Professor, Department of Development Engineering and Materials Science, Faculty of Engineering.
†Department of Development Engineering and Materials Science.
‡Associate Professor, Department of Structural Engineering.

range. The similar conclusions were obtained at a later time by Sweet et al.,[6] Goldschmied and Wormley,[7] and Hinchey and Sullivan.[8,9] The unsteady operating characteristics of fans were considered,[7,8] using the linear theory that was originally developed by Ohashi[10] for the analysis of turbopumps. It was suggested that the dynamic effect was negligible except for the high-frequency range over 20 Hz. Hinchey and Sullivan[9] solved the one-dimensional and unsteady flow in the ducting. The static fan characteristics were used. It was reported that the inertance of the air in the ducting was important even for relatively short ducts. Goldschmied and Wormley[7] as well as Hinchey and Sullivan[9] solved one-dimensional acoustic equations for the duct flow and suggested that the wave-propagation phenomena were only significant in the high-frequency range. Particularly, Hinchey and Sullivan[9] pointed out that the phenomena appeared in the frequency range over 5 Hz. Durkin and Luehr[11] investigated the dynamic characteristics of the volute fan by considering the unsteady and incompressible flow in the volute. Hinchey and Sullivan[12,13] investigated the limit cycle oscillations that frequently appeared in skirted air cusions. Recently, Sullivan et al.[14] have considered the effect of flexible trunks, assuming that they make a perfect seal once they contact the ground plane.

These preceding studies now suggest that, in the moderate frequency range below 10 Hz, dominant unsteady effects would be those appearing in the duct flow, that is, the lumped-inertance effect and the wave-propagation phenomena. In the present analysis, these effects are considered by combining the solution of the one-dimensional unsteady and compressible flow in the ducting with the characteristics of the power plant, the fan, and the cushion. The numerical results suggest that the wave effect becomes conspicuous in the large-amplitude–high-frequency oscillation and tends to relax the lumped-inertance effect. The results are also compared with those obtained by the forced-oscillation test. Considering the wave effect improves the theoretical result in the large-amplitude–high-frequency oscillation. The equation of motion of the vehicle has not been considered here to separate the additional factors arising from it. The analysis of the dynamics of the fan-duct-plenum system is prerequisite to the stability analysis of unskirted air cusions in oscillation without the riding-surface contact. Once it is established, it would be easily combined with the equation of motion. For flexible-skirted air cusions (particularly when the surface contact occurs), there still remain important aerohydroelastic problems, which should be treated separately.

II. Theoretical Formulations

A sketch of an air cusion in heaving motion is shown in Fig. 1. The air comes through the fan and is supplied to the cushion via the ducting. The air is considered to be inviscid and compressible. The cushion is assumed to be in the reservoir condition. For the continuity of the flow into and out of the cushion, we have

$$\frac{d}{dt}(\rho V)_{\text{cushion}} = M_{\text{in}} - M_{\text{out}} \tag{1}$$

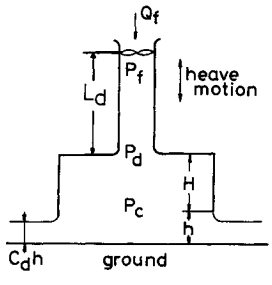

Fig. 1 Theoretical model of a fan-duct-plenum system.

Assuming that the flow is isentropic, we have

$$P_d\rho_d^{-\gamma} = P_c\rho_c^{-\gamma} = P_0\rho_0^{-\gamma}$$

An alternative assumption, $P_d = P_c$, has occasionally been made.[14] This implies that the air in the cushion has a flow velocity, or otherwise the kinetic energy in the ducting is dissipated.

Now we have

$$V = S(H + h)$$

$$M_{\text{in}} = \rho_d u_d S_f$$

$$M_{\text{out}} = K\rho_0 C C_d h \sqrt{\frac{2\gamma}{\gamma - 1}\frac{P_c}{\rho_c}\left\{1 - \left(\frac{P_0}{P_c}\right)^{(\gamma-1)/\gamma}\right\}}$$

The coefficient K is defined as follows:

$$K = 1 \qquad \text{for} \qquad P_0/P_c \le 1$$

$$K = -1 \qquad \text{for} \qquad P_0/P_c > 1$$

The full compressible law is retained here, since it does no harm to the analysis of small cushion pressure cases and even permits the extended application to large cushion pressure cases.

Substituting these expressions into Eq. (1), we obtain

$$\frac{(H+h)}{\gamma P_C}S\dot{P}_C + S\dot{h} = \left(\frac{P_0}{P_c}\right)^{1/\gamma}\left\{\left(\frac{P_d}{P_0}\right)^{1/\gamma}u_d S_f - KCC_d h \times\sqrt{\frac{2\gamma}{\gamma-1}\frac{P_c}{\rho_0}\left(\frac{P_0}{P_c}\right)^{1/\gamma}\left[1 - \left(\frac{P_0}{P_c}\right)^{(\gamma-1)/\gamma}\right]}\right\} \tag{2}$$

where the overdot represents the differentiation with respect to time. Equation (2) describes the operation condition of the cushion.

Assuming that the fan and the power plant operate quasistatically, we have

$$P_f = P_f(Q_f, n_f) \tag{3}$$

$$T_f = T_f(Q_f, n_f) \tag{4}$$

$$T_p = T_p(n_p, \phi) \tag{5}$$

The equations of motion of rotating parts of the fan and the power plant are respectively written as follows:

$$J_f\dot{n}_f = T_{sf} - T_f \tag{6}$$

$$J_p\dot{n}_p = T_p - T_{sp} \tag{7}$$

where T_{sf} and T_{sp} are the actual torques affected by the rotary inertia and $J_f/(2\pi)$ and $J_p/(2\pi)$ are the moments of inertia of the fan and the power plant, respectively. We thus have the relations

$$n_p = \kappa n_f \tag{8}$$

$$T_{sf} = \kappa\eta_t T_{sp} \tag{9}$$

Equations (3–9) describe the operating condition of the fan and the power plant.

We assume that the flow in the ducting is one-dimensional and isentropic; then the conservation laws are written in the

characteristic form as follows:

$$\frac{du}{dt} + \frac{2a}{\gamma - 1}\frac{da}{dt} + \frac{2\beta}{d}u|u| = 0 \quad \text{along} \quad \frac{dx}{dt} = u + a \tag{10}$$

$$\frac{du}{dt} - \frac{2a}{\gamma - 1}\frac{da}{dt} + \frac{2\beta}{d}u|u| = 0 \quad \text{along} \quad \frac{dx}{dt} = u - a \tag{11}$$

where the x axis is taken along the duct length ($x = 0$ at the duct entrance and $x = L_d$ at the duct exit). The β is related to the duct loss coefficient as follows:

$$\zeta = 4\beta L_d/d$$

The a is represented in terms of P as

$$a = a(P) = \gamma^{1/2}(P_0/\rho_0^{\gamma})^{1/2\gamma}P^{(\gamma-1)/2\gamma}$$

Equations (10) and (11) are solved with appropriate initial and boundary conditions.

Assuming that the flow changes isentropically from the duct exit into the cushion and the reservoir condition is eventually attained, then we have

$$P_c^{(\gamma-1)/\gamma} = P_d^{(\gamma-1)/\gamma} + [(\gamma - 1)/2\gamma]\rho_0 P_0^{-1/\gamma}u_d^2 \tag{12}$$

We also have the relations

$$P_f = P_i \tag{13}$$

$$Q_f = S_f u_i \tag{14}$$

Equations (2–14), together with the isentropic relation and the equation of sound speed, constitute a system of differential equations that govern the dynamics of the system. The parameter ϕ is usually kept fixed during the oscillation.

Eliminating T_{sf}, T_{sp}, and n_p between Eqs. (6) and (7) with the aid of Eqs. (8) and (9), we obtain

$$(J_f + \kappa^2\eta_t J_p)\dot{n}_f + T_f - \kappa\eta_t T_p = 0 \tag{15}$$

Substituting Eqs. (4), (5), (8), and (14) into Eq. (15), we have

$$(J_f + \kappa^2\eta_t J_p)\dot{n}_f + T_f(S_f u_i, n_f) - \kappa\eta_t T_p(\kappa n_f, \phi) = 0 \tag{16}$$

From Eqs. (3), (13), and (14), we have

$$P_i = P_f(S_f u_i, n_f) \tag{17}$$

The basic equations are now summarized as follows:

$$f_1(\dot{P}_c, P_c, P_d, u_d; \dot{h}, h) = 0 \tag{18}$$

$$f_2(P_c, P_d, u_d) = 0 \tag{19}$$

$$f_3(u, P) = 0 \quad \text{along} \quad \frac{dx}{dt} = u + a(P) \tag{20}$$

$$f_4(u, P) = 0 \quad \text{along} \quad \frac{dx}{dt} = u - a(P) \tag{21}$$

$$f_5(\dot{n}_f, n_f, \dot{u}_i) = 0 \tag{22}$$

$$f_6(n_f, P_i, u_i) = 0 \tag{23}$$

where

$$f_1 = \frac{S(H + h)}{\gamma P_c}\dot{P}_c + S\dot{h} - \left(\frac{P_0}{P_c}\right)^{1/\gamma}\left\{\left(\frac{P_d}{P_0}\right)^{1/\gamma}u_d S_f - KCC_d h \times \sqrt{\frac{2\gamma}{\gamma - 1}\frac{P_c}{\rho_0}\left(\frac{P_0}{P_c}\right)^{1/\gamma}\left[1 - \left(\frac{P_0}{P_c}\right)^{(\gamma-1)/\gamma}\right]}\right\}$$

$$f_2 = P_C^{(\gamma-1)/\gamma} - P_d^{(\gamma-1)/\gamma} - [(\gamma - 1)2\gamma]\rho_0 P_0^{-1/\gamma}u_d^2$$

$$f_3 = \frac{du}{dt} + \frac{2a(P)}{\gamma - 1}\frac{da}{dt} + \frac{2\beta}{d}u|u|$$

$$f_4 = \frac{du}{dt} - \frac{2a(P)}{\gamma - 1}\frac{da}{dt} + \frac{2\beta}{d}u|u|$$

$$f_5 = (J_f + \kappa^2\eta_t J_p)\dot{n}_f + T_f(S_f u_i, n_f) - \kappa\eta_t T_p(\kappa n_f, \phi)$$

$$f_6 = P_i - P_f(S_f u_i, n_f)$$

We shall assume that $h(t)$ is now prescribed and the initial data are given along the duct length as well as the boundary values u_d, P_d, u_i, and P_i at both ends. The initial values of P_c and n_f are then obtained from Eqs. (19) and (23), respectively. The values of P_c and n_f at the next time step are obtained by solving the differential Eqs. (18) and (22), respectively. The solutions of Eqs. (20) and (21) give the distributions of u and P along the duct length at the next time step except for the boundary values at both ends. The boundary values P_d and u_d at the next time step are obtained by combining Eqs. (19) and (20). Similarly, P_i and u_i at the next time step are obtained from Eqs. (21) and (23). A variety of examples to solve similar problems is given in Ref. 15. However, details are described in the Appendix to clarify the numerical procedure for obtaining the boundary values for this particular problem.

III. Numerical Calculations

We shall assume a simple harmonic oscillation represented by

$$h = h_e + \Delta h \sin(2\pi ft) \tag{24}$$

Operating characteristics of the fan have been represented in nondimensional form as follows:

$$\psi = \psi(\xi) \tag{25}$$

$$\lambda = \lambda(\xi) \tag{26}$$

whereas

$$\xi = 4Q_f/(\pi^2 d^3 n_f) = 4S_f u_i/(\pi^2 d^3 n_f) \tag{27}$$

$$\psi = 2P_f/(\rho_0\pi^2 d^2 n_f^2) = 2P_i/(\rho_0\pi^2 d^2 n_f^2) \tag{28}$$

$$\lambda = 16T_f/(\rho_0\pi^3 d^5 n_f^2) \tag{29}$$

where d is the diameter of the fan. Equation (3) or (23) is now replaced by Eq. (25). The $\psi(\xi)$ was approximated by a second-degree polynomial in ξ and $\lambda(\xi)$ by a third-degree polynomial. Similarly, $T_p(n_p)$ was approximated by a fourth-degree polynomial in n_p. Functions $\psi(\xi)$ and $\lambda(\xi)$ are graphically represented in Fig. 2 and $T_p(n_p)$ in Fig. 3.

Differential equations [Eqs. (18) and (22)] were numerically solved using the fourth-order Runge-Kutta method. Equations (20) and (21) were solved by the Hartree's method with the fixed time interval Δt, the value of which was determined at

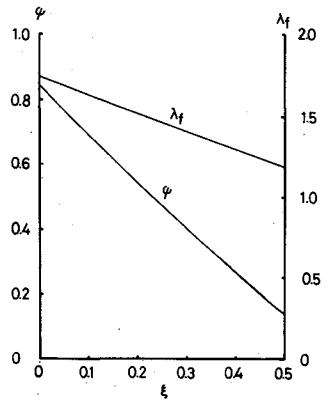

Fig. 2 Nondimensional characteristic variables of fan: $\psi(\xi)$ and $\lambda(\xi)$.

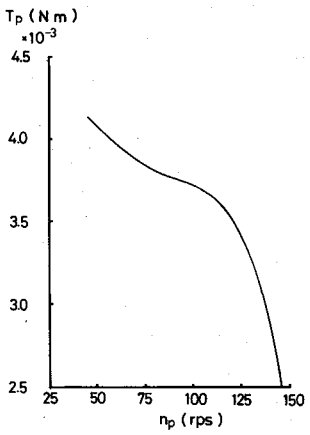

Fig. 3 Output torque of powerplant (electric motor): $T_p(n_p)$.

each time step by the Courant-Friedrichs-Lewy condition

$$\Delta t \leq \Delta x/(a + |u|) \tag{30}$$

The value of Δx was taken as 2% of the duct length.

The numerical integration of the system of the basic equations was continued until the steady-state condition that was independent of the initial condition was attained.

Numerical values used in the calculation are as follows:

$C_d = 0.635$, $h_e = 5$ mm

$C = 0.4$ m, $d = 0.062$ m

$H = 0.39$ m, $L_d = 4.19$ m

$S = 0.04$ m^2, $S_f = 0.00302$ m^2

$\rho_0 = 1.2054$ kg/m^3, $P_0 = 101.234$ kPa

$J_f = 2.16 \times 10^{-2}$ kg/m^2, $J_p = 1.177 \times 10^{-6}$ kg/m^2

$\gamma = 1.4$, $\kappa = 1$

$\eta_t = 1$, $\zeta = 2.4$

The stationary condition at h_e was chosen as the initial condition. The initial values at $t = 0$ are then given as

$$h = h_e = 5 \text{ mm}, \quad P_d = P_0 + 81.9 \text{ Pa}, \quad P_i = P_0 + 139.7 \text{ Pa}$$

$$P = P_i + (P_d - P_i)x/L_d, \quad u = u_d = u_i = 5.400 \text{ m/s}$$

on $0 \leq x \leq L_d$

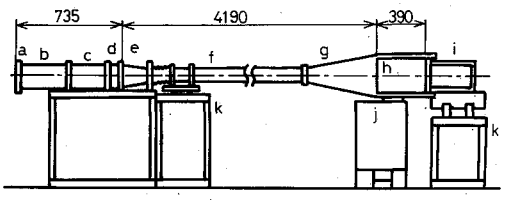

Fig. 4 A sketch of experimental setup. a) Inlet nozzle; b,c) intake duct; d) fan shroud; e,f,g) ducting; h) air cushion; i) ground plate support; j) oscillation device; k) support.

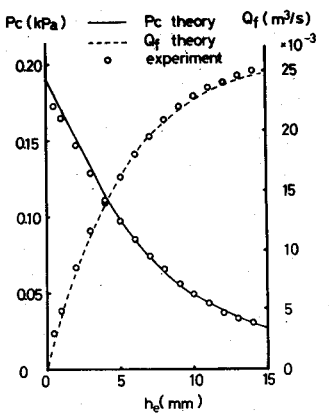

Fig. 5 Cushion pressure and fan volume flow rate at stationary condition.

Calculations were made for various amplitude ratios ($\Delta h/h_e$) and f.

The numerical data selected are in accordance with those of the forced-oscillation test model. A sketch of the experimental setup is shown in Fig. 4. The duct and plenum system oscillates horizontally. The sinusoidal oscillation below 10 Hz can be imposed. The instantaneous cushion pressure and hoverheight are measured electrically. The duct length is taken as long as possible to lower the critical frequency at which the wave effect begins to appear. An empirical formula is given in Ref. 15 to estimate the critical frequency, which is estimated as 3.2 Hz in the present case.

IV. Results and Discussion

The stationary condition with a fixed hoverheight is a particular case of the oscillating condition. It is then similarly analyzed using the same basic equations. The cushion pressure and the volume flow rate of the fan at the stationary condition are shown in Fig. 5. Experimental results are also plotted. The theoretical and experimental results are nearly identical. The variation of the fan rotating speed is shown in Fig. 6 against the stationary hoverheight. The agreement between the two results is also excellent. These results suggest that the present method might be reasonably extended to the analysis of the oscillating condition.

The variation of the cushion pressure with the progress of time is shown in Figs. 7 and 8. The numerical result is shown together with the result of the inertance model analysis. The experimental results are also shown. The wave effect in the small-amplitude oscillation (Fig. 7; $\Delta h/h_e = 1/5$) is almost negligible both in the lower- and higher-frequency range. Two theoretical results nearly agree with the experimental result. In the large-amplitude oscillation (Fig. 8; $\Delta h/h_e = 4/5$), the inertance model produces too large of a cushion pressure. The difference in the phase is also noticeable. Considering the wave effect relaxes the inertial effect. The cushion pressure then approaches the experimental value. The difference in the phase is also reduced. In fact, the relaxation mechanism would

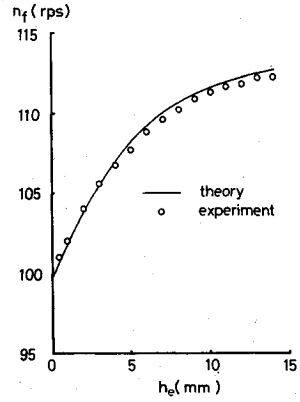

Fig. 6 Variation of fan rotating speed at stationary condition.

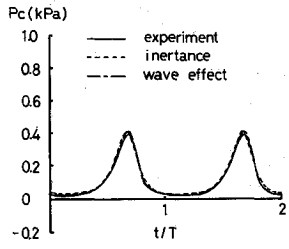

Fig. 7 Variation of cushion pressure with the progress of time: $f = 6$ Hz, $\Delta h/h_e = 1/5$; T represents period of oscillation.

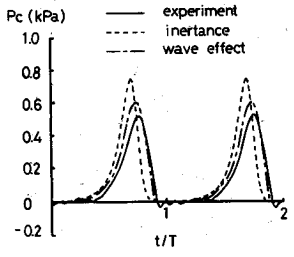

Fig. 8 Variation of cushion pressure with the progress of time: $f = 6$ Hz, $\Delta h/h_e = 4/5$; T represents period of oscillation.

be explained as follows: Suppose, for example, an instant when the hoverheight is reducing. To be compatible with the decrease of the mass in the cushion cavity, the gap flow beneath the nozzle exit must increase. However, the gap distance, i.e., the hoverheight, is now adversely reduced. The self-compensation is then only achieved by the instantaneous increase of the cushion pressure. This disturbance would have a choking effect on the outflow from the duct exit and tend to retard it. However, the inertance of the air in the ducting overcomes the effect and the change in the flow rate is suppressed. This would cause a larger flow rate and consequently a larger cushion pressure than in the flow without inertia. When the compressibility is present, the outflow from the duct instantly responds to the disturbance in a small region near the exit. The flow is now locally retarded. This would cause a smaller cushion pressure than in the incompressible fluid with inertance.

The peak values of the cushion pressure appearing in the pressure variation curves as given in Figs. 7 and 8 are plotted in Fig. 9 against the oscillation frequency. In the small-amplitude oscillation, the result from the lumped-inertance model agrees with that involving the wave effect. In this case the wave effect is almost negligible, even in the higher-frequency oscillation. In the large-amplitude oscillation, the wave effect tends to relax the inertial effect and to lessen the peak value.

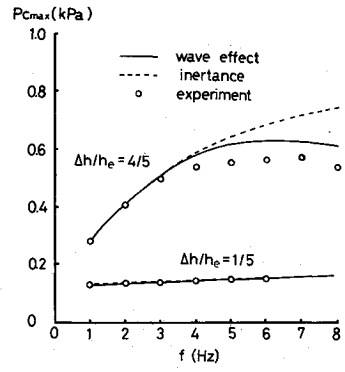

Fig. 9 Peak values of cushion pressure vs oscillation frequency.

The tendency is more noticeable in the higher-frequency range. The critical frequency at which the wave effect becomes conspicuous lies in f of 3–4 Hz. Using an empirical formula given in Ref. 15, it is calculated as 3.2 Hz. It can also be seen that the peak value takes an extremal value near f of 6 Hz. The similar tendency is observed in the experimental result. This suggests that the wave effect comes out more and more predominantly as the frequency increases.

V. Conclusion

The dynamic response of the fan-duct-plenum system is analyzed considering the wave propagation in the duct flow. A sinusoidal exit area modulation is imposed. In the small-amplitude oscillation, the result agrees with that obtained from the lumped-inertance model. In the large-amplitude-high-frequency oscillation, the wave effect relaxes the inertial effect. The frequency response of the cushion pressure is also investigated. The response curve has an extremal point in the lower-frequency range. It suggests that the wave effect comes out more and more predominant as the frequency increases. The numerical results are compared with those of the forced-oscillation test. It is shown that the theoretical analysis is improved by considering the wave effect.

Appendix

Draw a characteristic from point A, the boundary point at the next time step $t + \Delta t$ (see Fig. A1), and find the point of intersection B on the initial line; then, from Eq. (20), we have

$$P_d = P_B\left[\frac{\gamma-1}{2a(P_B)}(u_B - u_d) + 1 - \frac{\beta(\gamma-1)}{da(P_B)}u_B|u_B|\Delta t\right]^{2\gamma/(\gamma-1)} \tag{A1}$$

where the subscript B indicates the initial data at point B. Substituting Eq. (A1) into Eq. (19) and solving for u_d, we have

$$u_d = [\alpha_2 - (\alpha_2^2 - 4\alpha_1\alpha_3)^{1/2}]/2\alpha_1 \tag{A2}$$

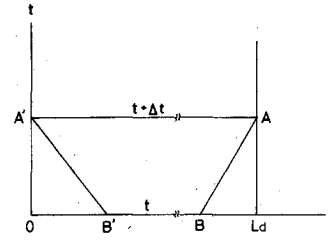

Fig. A1 Determination of boundary values.

where

$$\alpha_1 = P_B^{(\gamma-1)/\gamma}\left[\frac{\gamma-1}{2a(P_B)}\right]^2 + \frac{\gamma-1}{2\gamma}\rho_0 P_0^{-1/\gamma}$$

$$\alpha_2 = P_B^{(\gamma-1)/\gamma}\left\{\left[\frac{\gamma-1}{2a(P_B)}\right]^2 2u_B + \frac{\gamma-1}{a(P_B)} \times \left[1 - \frac{\beta(\gamma-1)}{da(P_B)}u_B|u_B|\Delta t\right]\right\}$$

$$\alpha_3 = P_B^{(\gamma-1)/\gamma}\left\{\left[\frac{\gamma-1}{2a(P_B)}\right]^2 u_B^2 + \frac{\gamma-1}{a(P_B)}u_B \times \left[1 - \frac{\beta(\gamma-1)}{da(P_B)}u_B|u_B|\Delta t\right] + \left[1 - \frac{\beta(\gamma-1)}{da(P_B)}u_B|u_B|\Delta t\right]^2\right\} - P_c^{(\gamma-1)/\gamma}$$

Equation (A1), together with Eq. (A2), prescribes the boundary values at the next time step.

Similarly, we have from Eq. (21)

$$P_i = P_{B'}\left[\frac{\gamma-1}{2a(P_{B'})}(u_i - u_{B'}) + 1 + \frac{\beta(\gamma-1)}{da(P_{B'})}u_{B'}|u_{B'}|\Delta t\right]^{2\gamma/(\gamma-1)} \tag{A3}$$

where the subscript B' indicates the values at the point B', the point of intersection of the characteristic drawn from another boundary point A' with the initial line (Fig. A1).

Dividing the both sides of Eq. (A3) by $\rho_0\pi^2 d^2 n_f/2$, we have

$$\frac{2P_{B'}}{\rho_0\pi^2 d^2 n_f^2}\left[\frac{\gamma-1}{2a(P_{B'})}(u_i - u_{B'}) + 1 + \frac{\beta(\gamma-1)}{da(P_{B'})}u_{B'}|u_{B'}|\Delta t\right]^{2\gamma/(\gamma-1)} \tag{A4}$$

Eliminating ψ between Eqs. (A4) and (25), the latter of which is now the alternative to Eq. (23), we have

$$\frac{2P_{B'}}{\rho_0\pi^2 d^2 n_f^2}\left[\frac{\gamma-1}{2a(P_{B'})}(u_i - u_{B'}) + 1 + \frac{\beta(\gamma-1)}{da(P_{B'})}u_{B'}|u_{B'}|\Delta t\right]^{2\gamma/(\gamma-1)} = \psi(\xi) = \psi\left(\frac{4S_f u_i}{\pi^2 d^3 n_f}\right) \tag{A5}$$

If the function $\psi(\xi)$ is known, u_i is obtained by solving Eq. (A5) for u_i. Actually, it was made by iteration using the dissection method. The iteration was repeated until the relative error in the value of u_i was less than 10^{-6}.

References

[1]Matsuo, H. and Matsuo, K., "Effects of Fan, Ducting and Powerplant Characteristics on Cushion Stability of Air Cushion Vehicles," *Journal of Aircraft,* Vol. 18, May 1981, pp. 372–376.

[2]Matsuo, H. and Matsuo, K., "A Nonlinear Analysis of Cushion Stability of ACV's in Vertical Motion," *Journal of the Japan Society for Aeronautical and Space Sciences,* Vol. 31, July 1983, pp. 376–384 (in Japanese).

[3]Matsuo, H. and Matsuo, K., "A Nonlinear Analysis of the Cushion Stability of Slowly Oscillating ACV's," *Journal of Aircraft,* Vol. 21, July 1984, pp. 539–541.

[4]Matsuo, H. and Matsuo, K., "A Nonlinear Analysis of Cushion Stability of ACV's in Vertical Motion (Continued Report)," *Journal of the Japan Society for Aeronautical and Space Sciences,* Vol. 33, Aug. 1985, pp. 484–490 (in Japanese); see also Matsuo, H. and Matsuo, K., "Nonlinear Analysis of Cushion Stability of ACV's in Heave," *Transactions of the Japan Society for Aeronautical and Space Sciences,* Vol. 29, Feb. 1987, pp. 220–229.

[5]Yano, R. and Nagayama, F., "Study of Surging in the Scavenging System of the Diesel Engine," *Journal of the Japan Society of Mechanical Engineering,* Pt. 2, Vol. 36, Aug. 1970, pp. 1374–1384 (in Japanese).

[6]Sweet, L. M., Richardson, H. H., and Wormley, D. N., "Plenum Air Cushion/Compressor-Duct Dynamic Interactions," *Journal of Dynamic Systems, Measurement, and Control,* Vol. 97, Sept. 1975, pp. 283–292.

[7]Goldschmied, F. R. and Wormley, D. N., "Frequency Response of Blower-Duct-Plenum Systems," *Journal of Hydronautics,* Vol. 11, Jan. 1977, pp. 18–27.

[8]Hinchy, M. J. and Sullivan, P. A., "Duct Effects on the Heave Stability of Plenum Air Cushion," *Journal of Sound and Vibration,* Vol. 60, Sept. 1978, pp. 87–99.

[9]Hinchy, M. J. and Sullivan, P. A., "Duct Effects on the Dynamic Fan Characteristics of Air Cushion Systems," *Journal of Hydronautics,* Vol. 13, Jan. 1979, pp. 28–29.

[10]Ohashi, H., "Experimental Study of the Dynamic Characteristics of Turbopumps," NASA TMX-53659, 1967.

[11]Durkin, J. M. and Luehr, L. W. H., "Dynamic Response of Lift Fans Subject to Varying Backpressure," AIAA Paper 78-756, April 1978.

[12]Hinchy, M. J. and Sullivan, P. A., "A Theoretical Study of Limit Cycle Oscillations of Plenum Air Cushions," *Journal of Sound and Vibration,* Vol. 79, Jan. 1981, pp. 61–77.

[13]Hinchy, M. J. and Sullivan, P. A., "Hovercraft Heave Stability," *Canadian Aeronautics and Space Journal,* Vol. 30, June 1984, pp. 130–151.

[14]Sullivan, P. A., Byrne, J. E., and Hinchey, M. J., "Non-linear Oscillations of a Simple Flexible Skirt Air Cushion," *Journal of Sound and Vibration,* Vol. 102, Feb. 1985, pp. 269–283.

[15]Wylie, E. B. and Streeter, V. L., *Fluid Transients,* McGraw-Hill, New York, 1978.